



Application of graphene to modified ionic liquid graphite composite and its enhanced electrochemical catalysis properties for levodopa oxidation

Mohammad Mazloun-Ardakani*, Alireza Khoshroo, Laleh Hosseinzadeh

Department of Chemistry, Faculty of Science, Yazd University, Yazd 89195-741, Iran

ARTICLE INFO

Article history:

Received 20 March 2014

Received in revised form 24 June 2014

Accepted 20 July 2014

Available online 26 July 2014

Keywords:

Levodopa

Graphene

Ionic liquid

Electrocatalysis

ABSTRACT

A novel kind of structurally uniform and electrocatalytic activity material formed by combination of graphene (GR), 1-(6,7-dihydroxy-2,4-dimethylbenzofuran-3-yl) ethanone (DE) and ionic liquid (IL) and used to modify carbon paste electrode (GR–DE–IL/CPE). The electrochemical properties of DE (as a modifier) in graphene paste electrode-based ionic liquids were studied in the aqueous solution. The fabricated GR–DE–IL/CPE was further used for the successful determination of levodopa (LD), and it exhibited an excellent electrocatalytic activity toward LD with a lower overvoltage, good electrochemical performances with higher conductivity and lower electron transfer resistance. It has been found that under optimum condition in CV, the oxidation of LD occurs at a potential about 400 mV less positive than that of an unmodified carbon paste electrode. Based on differential pulse voltammetry, the oxidation of LD exhibited a dynamic range between 0.015 and 1000 μ M and a detection limit (3σ) of 5.0 ± 1 nM. Finally, this method was used for the determination of LD in real samples, using standard addition method.

© 2014 Elsevier B.V. All rights reserved.

1. Introduction

Graphene (GR) has enjoyed significant recent attention [1–3]. Carbon-based nanostructures such as carbon nanofibers [4], carbon nanotubes (CNTs) [5], mesoporous carbons [6] and GR [7] have been extensively used in fabrication of modified electrodes for applications in both analytical and industrial electrochemistry, because in addition to their low price, they exhibit suitable electrocatalytic activity for a variety of redox reactions, a broad potential window, and relatively inert electrochemistry [8,9]. There is a significant challenge in the synthesis and application of graphene sheets. As a rising star of carbon nanomaterials, graphene sheets, two-dimensional sheets of sp^2 conjugated atomic carbon, have stimulated intense research interest because of they have a high specific surface area, unless well separated from each other, tend to form irreversible agglomerates or even restack to form graphite through strong π – π stacking and van der Waals interaction [10]. With unique structure and properties, GR naturally becomes a versatile nanoscale building block for self-assembly to achieve novel structures and functionalities.

Another important class of novel materials for various electrochemical applications is ionic liquids (IL), due to their unique chemical and physical properties. IL is a liquid electrolyte which consists of a small anion and a bulky organic cation such as imidazolium and pyridinium [11]. ILs can meet the challenge about graphene sheets well, due to their high surface area, excellent electrical conductivity, easy of synthesis, and good dispersibility and long-term stability in various solvents, GR/IL-based composite materials have been widely used in fabricating electrochemical sensors [12,13]. Different advantages could be achieved by using this composite electrode, such as (i) a remarkable increase in the rate of electron transfer of different organic and inorganic electroactive compounds, (ii) a marked decrease in the overvoltage for biomolecules, (iii) higher current density for a wide range of compounds tested were observed. All these properties allow a sensitive, low-potential, simple, low-cost, and stable composite electrode for the detection of biomolecules and other electroactive compounds [14,15].

There are four principle enhancement techniques for voltammetric and amperometric modified electrodes, namely selective preconcentration, permselectivity, selective recognition and electrocatalysis [16]. Electrocatalysis at chemically modified electrodes is widely utilized for the determination of many drugs and bio-substrates. Various inorganic and organic materials have been used to fabricate modified electrodes which can enhance the electron

* Corresponding author. Tel.: +98 3518211670; fax: +98 3518210644.

E-mail addresses: mazloun@yazd.ac.ir, mazlounardakani@gmail.com (M. Mazloun-Ardakani).

transfer rate and reduce the overpotential for the oxidation of substrates [17,18]. The chemical modification of electrodes using electron transfer mediators is an interesting field in analytical chemistry [19,20]. One of the most important effects of any mediator is a reduction of the overpotential required for electrochemical reaction, which enhances the sensitivity (current) and selectivity of the method [21].

To the best of our knowledge, there is no reported to application of graphene to modified carbon paste electrode with electron transfer mediators. Therefore, we used graphene for the construction of novel nanostructured benzofuran derivative (1-(6,7-dihydroxy-2,4-dimethylbenzofuran-3-yl) ethanone (DE)) modified ionic liquid-based carbon paste electrode (GR-DE-IL/CPE). The experimental results indicate that modified electrode offers several advantages such as high repeatability, good stability and high apparent charge transfer rate constant. Utilizing the developed method, determination of the levodopa has been carried out in urine and human blood serum samples.

2. Experimental

2.1. Instruments and reagents

The electrochemical measurements were performed with an Autolab potentiostat/galvanostat (PGSTAT-302N, EcoChemie, Netherlands). A conventional three-electrode cell was used at $25 \pm 1^\circ\text{C}$. An Ag/AgCl/KCl (3.0 M) electrode, a platinum wire, and modified carbon paste electrode (GR-DE-IL/CPE) were used as the reference, auxiliary and working electrodes, respectively. A Metrohm 691 pH/ion meter was used for pH measurements. Ultraviolet–visible (UV–Vis) spectra were obtained by an Optizen 3220UV UV–Vis spectrophotometer.

All solutions were freshly prepared with double distilled water. LD and all other reagents were of analytical grade from Sigma–Aldrich. Graphite powder and paraffin oil (DC 350, density = 0.88 g cm^{-3}), NH_3 , H_3PO_4 , H_2O_2 , ethanol, HCl, KMnO_4 , hydrazine monohydrate (N_2H_4 , 98%) and sulfuric acid were purchased from Merck. The buffer solutions were prepared from orthophosphoric acid and its salts in the pH range of 2.0–11.0.

2.2. Synthesis of 1-(6,7-dihydroxy-2,4-dimethylbenzofuran-3-yl) ethanone (DE)

DE was synthesized by electrosynthesis method according to the procedures described in the literature [22]. Briefly, 60 mL of 0.15 M sodium acetate in water, containing 1.0 mmol of 4-methylbenzene-1,2-diol and 1.0 mmol of acetylacetone was electrolyzed at controlled-potential (0.32 V) in a divided cell. The electrolysis was terminated when the current decayed to 5% of its initial value. At the end of electrolysis, a few drops of acetic acid were added to the solution and the cell was placed in a refrigerator overnight. The precipitated solid was collected by filtration and washed several times with water.

2.3. Synthesis of graphene sheets

Graphene oxide (GO) was obtained by oxidizing graphite using an improved method [23]. Briefly, a mixture of concentrated $\text{H}_2\text{SO}_4/\text{H}_3\text{PO}_4$ (360:40 mL) was added to a mixture of graphite/ KMnO_4 (3:18 g) at 50°C and stirred for 12 h. The reaction was cooled to room temperature and transferred onto flask ice with 30% H_2O_2 (3 mL). The obtained solution was centrifuged, and then filtered. The solid material was then washed with water, 30% HCl, and finally washed twice with 200 mL of ethanol.

We synthesized GR using hydrazine together with ammonia solution. A colloidal suspension of GO in purified water

(150 mg/50 mL) was prepared by sonication for 3 h. The suspension of GO was subsequently added to 50 μL of hydrazine solution (98%) with 200 μL of ammonia solution (30% in water). Then were refluxed at 90°C for 12 h in a heating mantle and cooled to room temperature. Subsequently solutions were centrifuged, and GR precipitates were washed with deionized water and then dried at 60°C in vacuum for 24 h.

2.4. Preparation of the electrode

To obtain the best conditions in the preparation of the GR-DE-IL/CPEs, we optimized the ratio of DE, GR and IL. The GR-DE-IL/CPEs were prepared by dissolving 0.006 g of DE in CH_3Cl and hand mixing with 0.55 g of graphite powder, 0.05 g of GR and 42 μL of IL using a mortar and pestle. Then $\sim 0.5\text{ mL}$ of paraffin was added to the above mixture and mixed for 20 min until a uniformly wetted paste was obtained. This paste was then packed into the end of a glass tube. A copper wire inserted into the carbon paste provided an electrical contact. When necessary, a new surface was obtained by pushing an excess of paste out of the tube and polishing with weighing paper. For comparison, DE modified CPE (DE/CPE) without GR and IL, DE and IL modified CPE (DE-IL/CPE) without GR, and unmodified carbon paste electrode in the absence of DE, GR and IL were also prepared in the same way.

3. Results and discussion

3.1. Characterization of graphene

The morphology of graphene was characterized by a scanning electron microscopy (SEM), infrared spectroscopy (IR) and ultraviolet–visible (UV–Vis). Typical SEM image of graphene was shown in Fig. 1A. In Fig. 1A, graphene exhibited a morphology consisting of a thin wrinkling paper-like structure. For comparison, SEM images of GO and graphite were shown in Fig. 1S, Supplementary material. Fig. 1B shows UV–Vis absorption spectra of GO before and after reduction using hydrazine. UV–Vis spectra of GO shows strong absorption band that could be attributed to $\pi \rightarrow \pi^*$ transitions of aromatic C=C bonds [24]. The UV–Vis spectra of this material suggest that the more ordered structure of GO is due to greater retention of carbon rings in the basal planes the two spectra were recorded for an equal concentration of each material (Fig. 1B). The degree of remaining conjugation can be determined by the λ_{max} of each UV–Vis spectrum. The more $\pi \rightarrow \pi^*$ transitions (conjugation), the less energy needs to be used for the electronic transition, which results in a higher λ_{max} [23]. The as-prepared GO displays two characteristics bands: a strong absorption band with a maximum at 228 nm and a shoulder at around 300 nm. Reduction of GO aqueous suspension resulted in a red shift of the main absorption band to 273 nm. In addition, the intensity of the absorption tail in the higher λ has significantly increased (Fig. 1B). The result suggests that the GO nanosheets have been reduced and the electronic conjugation within the GO nanosheet was restored upon hydrazine reduction [25].

Infrared spectroscopy (Fig. 1C) evidences for presence of $-\text{COOH}$, $-\text{OH}$ and $-\text{C}-\text{O}$ at GO sheet. The IR spectrum of GO shows a C–O stretch at 1222 cm^{-1} and O–H stretch at $3500\text{--}3300\text{ cm}^{-1}$ as well as a C=O stretch at $1720\text{--}1690\text{ cm}^{-1}$ [26]. After the final reduction with hydrazine, the absence of the peaks at $1720\text{--}1690$ and 1222 cm^{-1} indicates the epoxide and hydroxyl groups attached to the basal graphene layer have been removed (Fig. 1C).

3.2. Characteristics of the modified electrodes

The surface topography for GR/CPE showed a granular surface with the granules isolated and clearly distinguished (Fig. 2A). While

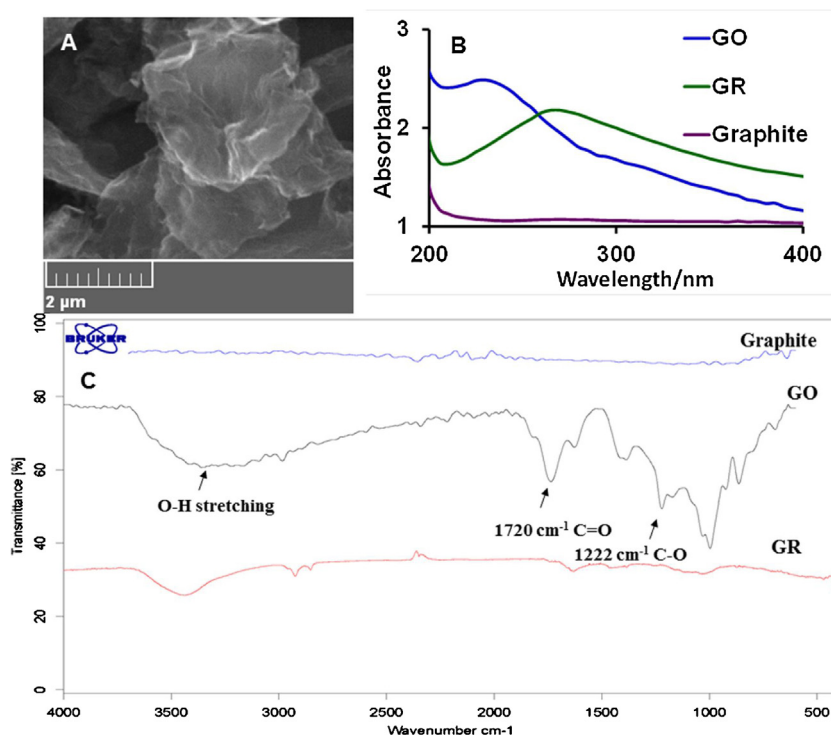


Fig. 1. Characterizations of GR. (A) SEM image, (B) UV-Vis absorption spectrum and (C) FTIR spectrum.

on GR-IL/CPE (Fig. 2B), a more uniform surface appeared without the separated carbon layers. A mass of IL was embedded between graphite particles, which bridged the granules and filled into the void spaces. Inset Fig. 2B is the enlarged magnification of GR-IL/CPE, it can be seen that the GR nanosheets and graphite interact together with ultrathin and homogeneous film, and the edges of individual sheets were distinguishable. This structure of GR is highly beneficial in maintaining a high surface area on the electrode and helpful in constructing an interface for the electrochemistry of organic modifier.

3.3. Electrochemical properties of GR-DE-IL/CPE

Electrochemical impedance spectroscopy (EIS) can exhibit the impedance changes during the modification processes, which is further used for the investigation on the electrode interface. The value of the electrode-transfer resistance (R_{ct}) depends on the dielectric and insulating features at the electrode/electrolyte interface with different modification processes. Fig. 3 shows the EIS of different modified electrodes in 10.0 mmol L⁻¹ K₃[Fe(CN)₆]/K₄[Fe(CN)₆] and 0.1 mol L⁻¹ KCl solution. On the CPE

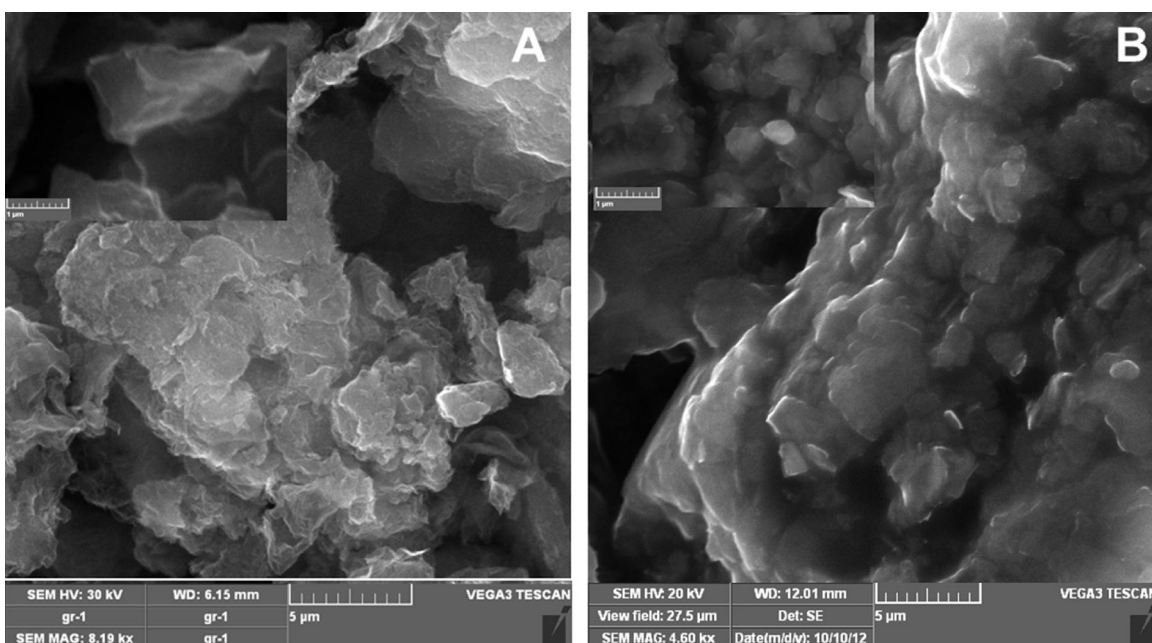


Fig. 2. SEM images of (A) GR-DE/CPE, (B) GR-DE-IL/CPE, and insets: high magnification of GR-DE/CPE and GR-DE-IL/CPE.

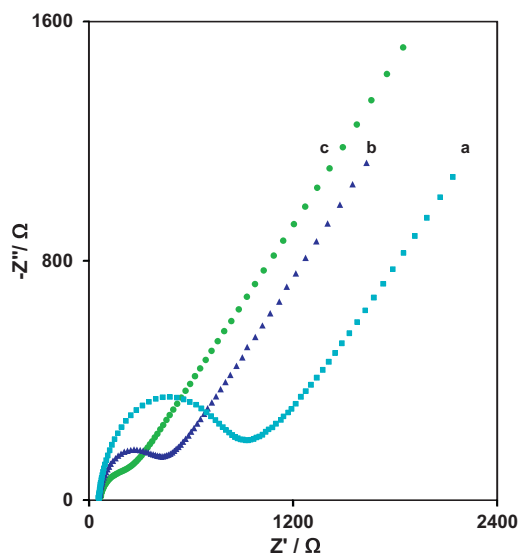


Fig. 3. (A) EIS of different modified electrodes in 10.0 mmol/L $[\text{Fe}(\text{CN})_6]^{3-/4-}$ containing 0.1 M KCl with the frequency from 10^4 to 1.0 Hz. From a to c were CPE, IL/CPE, GR-IL/CPE, respectively.

(curve a) the R_{ct} value was got as 950 Ω . While on IL/CPE (curve b) the R_{ct} values were decreased to 440 Ω , which was due to the presence of conductive IL in the carbon paste. The further decrease of interface electron impedance was obtained at GR-IL/CPE (curve c), indicating that high conductive GR nanosheets on the electrode surface could effectively increase the electron transfer rate between electrode surface and $[\text{Fe}(\text{CN})_6]^{3-/4-}$ ions due to the good conductivity of GR. Therefore, the electron transfer resistances of GR-IL/CPE (c) is remarkably lower than that of else electrodes, suggesting the synergistic effect of GR and IL on the modified electrode effectively enhanced the conductivity of the modified electrode and made it easier for the electron transfer from the electrode to the film.

Cyclic voltammetry (CV) was used for further characterization of the modified electrode. Fig. 4 demonstrates cyclic voltammetric behaviors of GR-DE-IL/CPE in buffered aqueous solution (pH = 7.0).

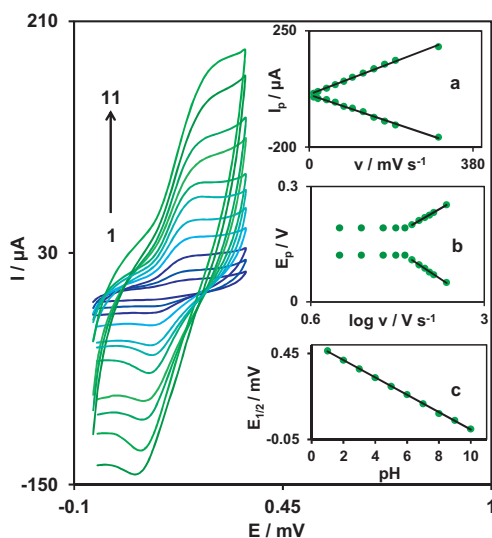


Fig. 4. Cyclic voltammograms of GR-DE-IL/CPE in 0.1 M phosphate buffer solution (pH 7.0) at different scan rates, from 1 to 11: 10, 20, 40, 60, 80, 100, 125, 150, 175, 200 and 300 mV s^{-1} , respectively; insets: variation of (a) I_p vs. scan rate; (b) E_p vs. the logarithm of scan rates; (c) $E_{1/2}$ vs. pH.

Experimental results showed well-defined, reproducible anodic and cathodic peaks with E_{pa} and E_{pc} of 0.19 and 0.12 V vs. Ag/AgCl (0.3 M), respectively. This result suggests that redox couple of DE in GR-DE-IL/CPE has a quasi-reversible behavior in aqueous medium. In addition, the effect of the potential scan rate (ν) on electrochemical properties of the GR-DE-IL/CPE was studied in an aqueous solution with CV. Plots of the anodic and cathodic peak currents (I_p) were linearly dependent on ν in the range of 10–300 mV s^{-1} , indicating that the redox process of DE at modified electrode is diffusionless in nature (inset a).

An approximate estimate of the surface coverage of the electrode was made by adopting the method used by Sharp et al. [27]. According to this method, the peak current is related to the surface concentration of electroactive species, Γ , by the following equation:

$$I_p = \frac{n^2 F^2 A \Gamma \nu}{4RT} \quad (1)$$

where n represents the number of electrons involved in reaction, A is the surface area (0.0962 cm^2) of the GR-DE-IL/CPE, Γ (mol cm^{-2}) is the surface coverage and other symbols have their usual meanings. From the slope of anodic peak currents versus scan rate (inset a) the calculated surface concentration of DE is $\Gamma = 1.78 \times 10^{-9} \text{ mol cm}^{-2}$ for $n = 2$.

The apparent charge transfer rate constant, k_s , and the charge transfer coefficient, α , of a surface-confined redox couple can be evaluated from CV experiments by using the variation of anodic and cathodic peak potentials with logarithm of scan rate, according to the procedure of Laviron [28]. Inset b shows such plots, indicating that the E_p values are proportional to the logarithm of scan rate for ν values higher than 0.08 V s^{-1} . The slopes of the plots in inset b can be used to extract the kinetic parameters α_c and α_a (cathodic and anodic transfer coefficients, respectively). The slopes of the linear segments are equal to $-2.303RT/\alpha nF$ and $2.303RT/(1-\alpha)nF$ for the cathodic and anodic peaks, respectively. The evaluated value for the α_a is 0.51.

Also, the following equation can be used to determine the electron transfer rate constant between modifier (DE) and electrode:

$$\log k_s = \alpha \log(1-\alpha) + (1-\alpha) \log \alpha - \log \left(\frac{RT}{nF\nu} \right) - \alpha(1-\alpha)nF \frac{\Delta E_p}{2.3RT} \quad (2)$$

where ν is the sweep rate and all other symbols having their conventional meanings. The value of $k_s = 26.1 \text{ s}^{-1}$ was evaluated using Eq. (2).

Also, the effect of GR and IL, used for fabrication of GR-DE-IL/CPE, on the k_s was investigated. They were 21.3 and 13.1 s^{-1} for GR-DE/CPE and DE/CPE, respectively. The k_s value significantly increases when GR and IL are used for fabrication of the modified electrode.

The electrochemical response of the DE molecule is generally pH dependent. Thus, the electrochemical behavior of the GR-DE-IL/CPE was studied at different pHs (1.0 < pH < 10.0) using CV. Anodic and cathodic peak potentials of the GR-DE-IL/CPE were shifted to less positive values with increases in pH. The half-wave potential of the GR-DE-IL/CPE at various pHs was calculated as the average value of the anodic and cathodic peak potentials of the CVs. A potential–pH diagram was constructed by plotting the calculated $E_{1/2}$ values as a function of pH (inset c). This diagram is composed of a straight line with slope = 50.60 mV/pH. Such behavior suggests that it obeys the Nernst equation for a two electron and proton transfer reaction [28].

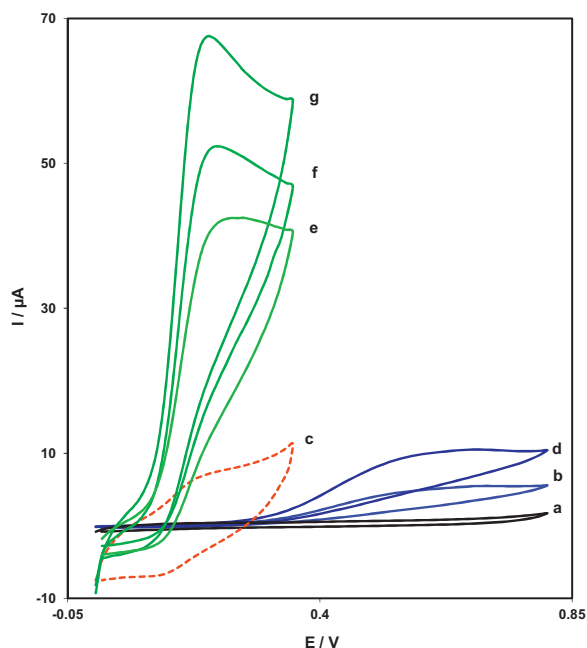


Fig. 5. CVs of (a) unmodified CPE in 0.1 M phosphate buffer solution (pH 7.0) at scan rate 20 mV s^{-1} ; (b) as (a) + 0.4 mM LD; (c) as (a) at the surface of GR-DE-IL/CPE; (d) as (b) at the surface of GR-IL/CPE; (e) as (b) at the surface of DE/CPE; (f) as (b) at the surface of DE-IL/CPE; (g) as (b) at the surface of GR-DE-IL/CPE.

3.4. Electrocatalytic characteristics of GR-DE-IL/CPE for oxidation of LD

Fig. 5 depicts the CV responses for the electrochemical oxidation of 0.4 mM LD at the GR-DE-IL/CPE (curve g), DE-IL/CPE (curve f), DE/CPE (curve e), and unmodified CPE (curve b). As shown, the anodic peak potential for LD oxidation at the GR-DE-IL/CPE (curve g) was about 200 mV, while at the unmodified CPE (curve b), the peak potential was about 600 mV. From these results, it was concluded that the best electrocatalytic effect for LD oxidation was observed at the GR-DE-IL/CPE (curve g). The comparison of the oxidation of LD at DE-IL/CPE (curve f) and DE/CPE (curve e) shows an enhancement of the anodic peak current at DE-IL/CPE, which indicated that the presence of ILs could enhance the peak currents. By mixing IL into carbon paste, a layer of IL is formed on the surface of graphite particles and the void spaces between graphite powders are filled, which increase the conductivity of DE-IL/CPE greatly. To investigate the roles of GR in GR-DE-IL/CPE in the electrochemical oxidation of LD, the CVs of LD at the GR-DE-IL/CPE (curve g) and DE-IL/CPE (curve f) were recorded. The results indicated that the presence of GR in modified electrode had great improvement on the electrochemical response. This might be related to the synergistic effect of graphene and IL. The high specific surface area and electrical conductivity of graphene and the unique properties of IL, such as high ionic conductivity and solubility toward various substrates, were helpful for promoting the electrochemical signals.

The GR-DE-IL/CPE, in 0.1 M phosphate buffer (pH 7.0) and without LD in solution, exhibited a well-behaved redox reaction (curve c), upon addition of 0.4 mM LD, there was a dramatic enhancement of the anodic peak current (curve g), indicating an EC' catalytic mechanism [8]. This mechanism is shown in Scheme S1, Supplementary material. In this scheme, LD is oxidized in the catalytic chemical reaction (C') by the oxidized form of DE (DE_{ox}) which produced via an electrochemical reaction (E). Therefore, the LD is oxidized at the potential of 200 mV at the GR-DE-IL/CPE while it is

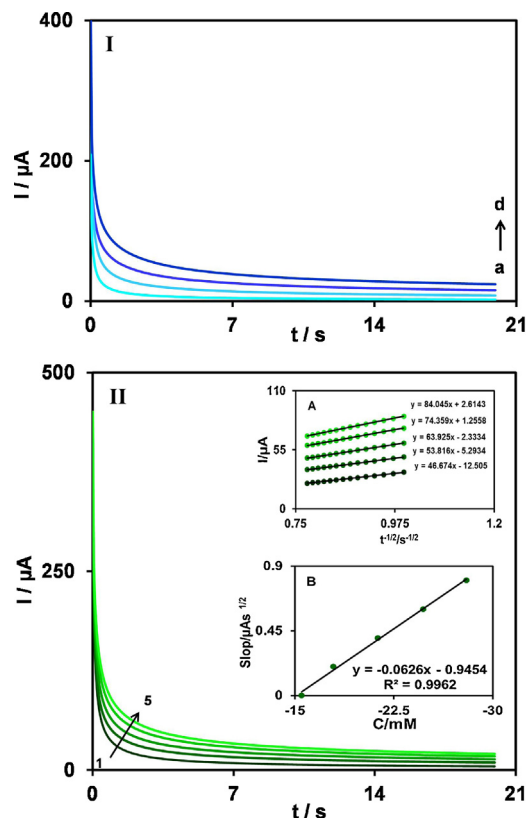


Fig. 6. (I) Chronoamperograms of LD oxidation on unmodified CPE (a), DE/CPE (b), DE-IL/CPE (c), GR-DE-IL/CPE (d) in the presence of 0.60 mM of LD, (II) chronoamperograms obtained at GR-DE-IL/CPE in 0.1 M phosphate buffer solution (pH 7.0) for different concentrations of LD. The numbers 1–5 correspond to 0.1, 0.2, 0.4, 0.6 and 0.89 mM of LD. Insets: (A) plots of I vs. $t^{1/2}$ obtained from chronoamperograms, (B) plot of the slope of the straight lines against the LD concentration.

oxidized at 600 mV at the carbon paste bare electrode (Fig. 5, curve b).

3.5. Chronoamperometric measurements

The chronoamperometry as well as the other electrochemical methods was employed for the investigation of electrode processes at chemically modified electrodes. The steady state behavior of LD oxidation on the surface of various modified electrode was studied by chronoamperometric. Fig. 6I shows the results of chronoamperometric measurements of unmodified CPE (a), DE/CPE (b), DE-IL/CPE (c) and GR-DE-IL/CPE (d) electrodes in 0.5 mM LD. All electrodes reach a steady-state Faradic current response within approximate 20 s. It was observed that the GR-DE-IL/CPE (d) electrode produces a higher steady state current density in comparison with that of the other electrode during the whole measurements. This could be attributed to the higher electrochemically active surface area of the GR-DE-IL/CPE which is in agreement with the results of cyclic voltammetry of LD oxidation.

Chronoamperometric measurements of LD at GR-DE-IL/CPE were carried out for various concentrations of LD (Fig. 6II). For an electroactive material (LD in this case) with a diffusion coefficient of D , the current observed for the electrochemical reaction at a mass transport limited condition is described by the Cottrell equation [8]. Inset B Fig. 6II shows the fitted experimental plots for different concentration of LD. The slopes of the resulting straight lines were then plotted vs. the LD concentration. From the resulting slope and Cottrell equation the mean value of the D was found to be $3.6 \times 10^{-5} \text{ cm}^2 \text{ s}^{-1}$.

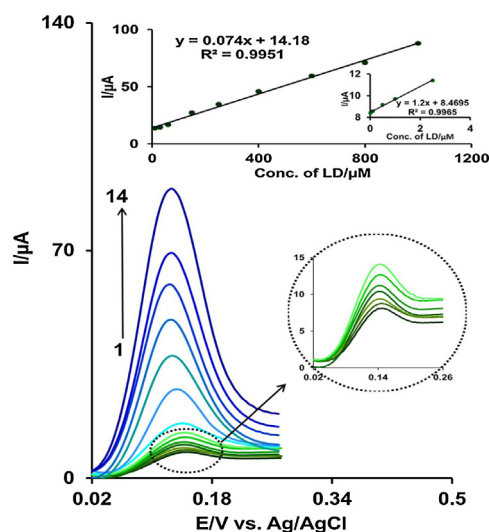


Fig. 7. DPVs of GR-DE-IL/CPE in 0.1 M phosphate buffer solution (pH 7.0) containing different concentrations of LD in μM ; the numbers 1–14 correspond to 0.015, 0.1, 0.5, 1, 2.5, 10, 30, 50, 150, 250, 400, 600, 800, 1000, respectively; insets: plots of the peak currents as a function of LD concentration.

3.6. Calibration plot and limit of detection

To evaluate the sensitivity and dynamic range of the GR-DE-IL/CPE, routine samples with various concentrations of LD were assayed under optimal conditions. As shown in Fig. 7, the DPV response of the sensor increased with the increment of LD concentration, and exhibited a very good linear relationship with the LD concentration from 0.015 to 1000.0 μM . The plot of peak current vs. LD concentration consisted of two linear segments with slopes of 1.2 and $0.074 \mu\text{A} \mu\text{M}^{-1}$ in the concentration ranges of 0.015–2.5 μM and 2.5–1000.0 μM , respectively. The decrease in sensitivity (slope) of the second linear segment is likely due to kinetic limitation. The detection limit (3σ) for LD in the lower range region was found to be $5.0 \pm 1 \text{ nM}$. Compared with other sensors reported previously (Table S1, Supplementary material), our proposed sensor exhibited a satisfactory detection limit and linear range.

3.7. Interference study

The influence of various foreign species on the determination of $1.0 \times 10^{-4} \text{ M}$ LD was investigated. The tolerance limit was taken as the maximum concentration of the foreign substances, which caused an approximately $\pm 5\%$ relative error in the determination. The tolerated concentration of foreign substances was $1.0 \times 10^{-1} \text{ M}$ for Cl^- , Na^+ , NO_3^- , F^- , S^{2-} , CO_3^{2-} , HCO_3^- and K^+ ; $5.0 \times 10^{-2} \text{ M}$ for Mg^{2+} , Ba^{2+} , Cd^{2+} , Cu^{2+} , Pb^{2+} , Ni^{2+} , Al^{3+} and Ca^{2+} ; $5.0 \times 10^{-3} \text{ M}$ for L-lysine, glucose, lactose, fructose, sucrose, L-cysteine, L-asparagines, L-glycine, L-glutamic acid, L-cystine, D-penicillamine, L-tryptophan, folic acid, uric acid and guanine.

3.8. Real sample analysis

The GR-DE-IL/CPE was successfully applied to the direct determination of the LD content of pharmaceutical samples (Parkin-C Fort, Madopar and Sinemet). The levodopa contents in these samples were determined by the standard addition method in order to prevent any matrix effect. The value of levodopa was found to be 240, 207 and 95 mg for Parkin-C Fort, Madopar and Sinemet samples respectively. The percentage difference between these results and the labeled values are 4.0%, 3.5% and 5% for levodopa,

Table 1

The application of GR-DE-IL/CPE for determination of LD in urine and human blood serum samples ($n = 7$).

Sample	Spiked (μM)	Found (μM)	Recovery (%)	RSD (%)
Urine				
1	0	ND	–	–
2	10	10.3	103.0	1.9
3	50	48.6	97.2	2.4
Human blood serum				
1	0	ND	–	–
2	10	9.6	96.0	2.4
3	50	51.2	102.4	3.1

respectively. The obtained values were in a good agreement with the labeled value. These results indicate that a GR-DE-IL/CPE could be applied for the routine analytical control of pharmaceuticals.

In order to evaluate the analytical applicability of the proposed method, also it was applied to the determination of LD in urine and human blood serum samples. The sample was found to be free from LD. Therefore different amounts of LD was spiked to the sample and analyzed by the proposed method. The results for determination of the LD in real samples are given in Table 1. Satisfactory recovery of the experimental results was found for LD. The reproducibility of the method was demonstrated by the mean relative standard deviation (RSD).

3.9. Reproducibility, stability and regeneration of the GR-DE-IL/CPE

The repeatability and stability of the proposed sensor were investigated in the presence of 30 μM by cyclic voltammetric measurements. The proposed sensor showed a repeatability with a relative standard deviation (RSD) of 2.1% for 20 successive assays. A RSD of 2.9% was obtained with five sensors prepared independently using the same procedure. The sensor retained more than 97.1% of its initial response to the oxidation of LD after a 4-week period storage.

4. Conclusions

In this paper, a novel CPE was successfully fabricated by using GR, DE and IL, which showed a high electrocatalytic activity and good selectivity toward the oxidation of LD. The CV and DPV investigations showed effective electrocatalytic activity of the modified electrode in lowering the anodic overpotential for the oxidation of LD. For first time, the electrochemical behavior of the mediator (DE) was studied in the presence of GR in modified IL/CPE. High sensitivity and selectivity of the voltammetric responses, and low detection limit ($5.0 \pm 1 \text{ nM}$), together with the ease of preparation and surface regeneration, make the proposed modified electrode very useful for accurate determination of LD in real samples.

Acknowledgements

The authors wish to thank the Yazd University Research Council, the IUT Research Council and Excellence in Sensors of Iran for financial support of this research.

Appendix A. Supplementary data

Supplementary data associated with this article can be found, in the online version, at <http://dx.doi.org/10.1016/j.snb.2014.07.069>.

References

- [1] G. Nanowalls, O. Akhavan, E. Ghaderi, R. Rahighi, A.E.T. Al, Toward single-DNA electrochemical biosensing by graphene nanowalls, *ACS Nano* 6 (2012) 2904–2916.
- [2] F. Li, J. Li, Y. Feng, L. Yang, Z. Du, Electrochemical behavior of graphene doped carbon paste electrode and its application for sensitive determination of ascorbic acid, *Sens. Actuators B: Chem.* 157 (2011) 110–114.
- [3] M. Wei, D. Tian, S. Liu, X. Zheng, S. Duan, C. Zhou, β -Cyclodextrin functionalized graphene material: a novel electrochemical sensor for simultaneous determination of 2-chlorophenol and 3-chlorophenol, *Sens. Actuators B: Chem.* 195 (2014) 452–458.
- [4] T.E. McKnight, A.V. Melechko, M.A. Guillorn, V.I. Merkulov, M.J. Doktycz, C.T. Culbertson, et al., Effects of microfabrication processing on the electrochemistry of carbon nanofiber electrodes, *J. Phys. Chem. B* 107 (2003) 10722–10728.
- [5] M. Mazloum-Ardakani, A. Khoshroo, High sensitive sensor based on functionalized carbon nanotube/ionic liquid nanocomposite for simultaneous determination of norepinephrine and serotonin, *J. Electroanal. Chem.* 717–718 (2014) 17–23.
- [6] X. Jiang, Y. Wu, X. Mao, X. Cui, L. Zhu, Amperometric glucose biosensor based on integration of glucose oxidase with platinum nanoparticles/ordered mesoporous carbon nanocomposite, *Sens. Actuators B: Chem.* 153 (2011) 158–163.
- [7] N. Jia, B. Huang, L. Chen, L. Tan, S. Yao, A simple non-enzymatic hydrogen peroxide sensor using gold nanoparticles–graphene–chitosan modified electrode, *Sens. Actuators B: Chem.* 195 (2014) 165–170.
- [8] A.J. Bard, L.R. Faulkner, *Electrochemical Methods: Fundamentals and Applications*, second ed., Wiley, New York, 2000.
- [9] M. Mazloum-Ardakani, M.A. Sheikh-Mohseni, M. Abdollahi-Alibeik, A. Benvidi, Electrochemical sensor for simultaneous determination of norepinephrine, paracetamol and folic acid by a nanostructured mesoporous material, *Sens. Actuators B: Chem.* 171–172 (2012) 380–390386.
- [10] D. Li, M.B. Müller, S. Gilje, R.B. Kaner, G.G. Wallace, Processable aqueous dispersions of graphene nanosheets, *Nat. Nanotechnol.* 3 (2008) 101–105.
- [11] D. Wei, A. Ivaska, Applications of ionic liquids in electrochemical sensors, *Anal. Chim. Acta* 607 (2008) 126–135.
- [12] M. Mazloum-Ardakani, A. Khoshroo, Nano composite system based on coumarin derivative–titanium dioxide nanoparticles and ionic liquid: determination of levodopa and carbidopa in human serum and pharmaceutical formulations, *Anal. Chim. Acta* 798 (2013) 25–32.
- [13] M. Mazloum-Ardakani, A. Khoshroo, An electrochemical study of benzofuran derivative in modified electrode-based CNT/ionic liquids for determining nanomolar concentrations of hydrazine, *Electrochim. Acta* 103 (2013) 77–84.
- [14] N. Maleki, A. Safavi, F. Tajabadi, High-performance carbon composite electrode based on an ionic liquid as a binder, *Anal. Chem.* 78 (2006) 3820–3826.
- [15] M. Mazloum-Ardakani, A. Khoshroo, High performance electrochemical sensor based on fullerene-functionalized carbon nanotubes/ionic liquid: determination of some catecholamines, *Electrochem. Commun.* 42 (2014) 9–12.
- [16] Y. Zhang, X. Chen, W. Yang, Direct electrochemistry and electrocatalysis of myoglobin immobilized in zirconium phosphate nanosheets film, *Sens. Actuators B: Chem.* 130 (2007) 682–688.
- [17] M. Mazloum-Ardakani, A. Khoshroo, An electrochemical study of benzofuran derivative in modified electrode-based CNT/ionic liquids for determining nanomolar concentrations of hydrazine, *Electrochim. Acta* 103 (2013) 77–84.
- [18] M. Mazloum-Ardakani, M. Abolhasani, B.-F. Mirjalili, M.A. Sheikh-Mohseni, A. Dehghani-Firouzabadi, A. Khoshroo, Electrocatalysis of dopamine in the presence of uric acid and folic acid on modified carbon nanotube paste electrode, *Chin. J. Catal.* 35 (2014) 201–209.
- [19] M. Mazloum-Ardakani, A. Naser-Sadrabadi, M.A. Sheikh-Mohseni, H. Naeimi, A. Benvidi, A. Khoshroo, Oxidized multiwalled carbon nanotubes for improving the electrocatalytic activity of a Schiff base modified electrode in determination of isoprenaline, *J. Electroanal. Chem.* 705 (2013) 75–80.
- [20] M. Mazloum-Ardakani, L. Hosseinzadeh, A. Khoshroo, H. Naeimi, M. Moradian, Simultaneous determination of isoproterenol, acetaminophen and folic acid using a novel nanostructure-based electrochemical sensor, *Electroanalysis* 26 (2014) 275–284.
- [21] M. Mazloum-Ardakani, Z. Taleat, A. Khoshroo, H. Beitollahi, H. Dehghani, Electrocatalytic oxidation and voltammetric determination of levodopa in the presence of carbidopa at the surface of a nanostructure based electrochemical sensor, *Biosens. Bioelectron.* 35 (2012) 75–81.
- [22] M. Mazloum-Ardakani, A. Khoshroo, D. Nematollahi, B.-F. Mirjalili, Electrochemical study of catechol derivatives in the presence of β -diketones: synthesis of benzofuran derivatives, *J. Electrochem. Soc.* 159 (2012) H912–H917.
- [23] D.C. Marcano, D.V. Kosynkin, J.M. Berlin, A. Sinitskii, Z. Sun, A. Slesarev, et al., Improved synthesis of graphene oxide, *ACS Nano* 4 (2010) 4806–4814.
- [24] Y. Hu, F. Li, D. Han, T. Wu, Q. Zhang, L. Niu, et al., Simple and label-free electrochemical assay for signal-on DNA hybridization directly at undecorated graphene oxide, *Anal. Chim. Acta* 753 (2012) 82–89.
- [25] Q. Wang, M.R. Das, M. Li, R. Boukherroub, S. Szunerits, Voltammetric detection of L-dopa and carbidopa on graphene modified glassy carbon interfaces, *Bioelectrochemistry* 93 (2013) 15–22.
- [26] J.R. Lomeda, C.D. Doyle, D.V. Kosynkin, W.-F. Hwang, J.M. Tour, Diazonium functionalization of surfactant-wrapped chemically converted graphene sheets, *J. Am. Chem. Soc.* 130 (2008) 16201–16206.
- [27] M. Sharp, M. Petersson, K. Edström, Preliminary determinations of electron transfer kinetics involving ferrocene covalently attached to a platinum surface, *J. Electroanal. Chem. Interfacial Electrochem.* 95 (1979) 123–130.
- [28] E. Laviron, General expression of the linear potential sweep voltammogram in the case of diffusionless electrochemical systems, *J. Electroanal. Chem. Interfacial Electrochem.* 101 (1979) 19–28.

Biographies

Mohammad Mazloum-Ardakani received BSc in chemistry from University of Kashan, Kashan, Iran, in 1986, and MSc in analytical chemistry from Teacher Training University, Tehran, Iran, in 1990, and his PhD in analytical chemistry from Isfahan University, Isfahan, Iran, in 2000. He is professor of analytical chemistry at the Chemistry Department in the Yazd University, Yazd, Iran. His main area of interest is electroanalytical chemistry, and nanoelectrochemistry.

Alireza Khoshroo received BSc in chemistry from Shahrood University of Technology, Shahrood, Iran, in 2008, and MSc in analytical chemistry from Yazd University, Yazd, Iran, in 2010, and since 2010 he is PhD student in analytical chemistry at Yazd University, Yazd, Iran. His current research interests are nanomaterial-based bio/chemical sensor development for determination of biocompounds and toxic compounds in the real samples and dye-sensitized solar cells development.

Laleh Hosseinzadeh received BSc in chemistry from Ilam University, Ilam, Iran, in 2006, and MSc in analytical chemistry from Ilam University, Ilam, Iran, in 2008, and since 2011 he is PhD student in analytical chemistry at Yazd University. His current research interests cover immunosensors, aptasensors and biosensor.